HHS Public Access

Author manuscript

Cancer Lett. Author manuscript; available in PMC 2019 October 01.

Published in final edited form as:

Cancer Lett. 2018 October 01; 433: 221–231. doi:10.1016/j.canlet.2018.07.003.

Prolactin signaling drives tumorigenesis in human high grade serous ovarian cancer cells and in a spontaneous fallopian tube derived model

Subbulakshmi Karthikeyan[a], **Angela Russo**[a], **Matthew Dean**[a], **Daniel D. Lantvit**[a], **Michael Endsley**[a,b], **Joanna E. Burdette**[a,*]

[a]Center for Biomolecular Sciences, Department of Medicinal Chemistry and Pharmacognosy, College of Pharmacy, University of Illinois at Chicago, Chicago, IL, 60607, USA

[b]Medical College of Wisconsin, Department of Obstetrics & Gynecology, 9200 West Wisconsin Ave, Milwaukee, WI, 53226-3522, USA

Abstract

The pathways responsible for tumorigenesis of high grade serous ovarian cancer (HGSOC) from the fallopian tube epithelium (FTE) are still poorly understood. A human prolactin (PRL) like gene, *Prl2c2* was amplified > 100 fold in a spontaneous model of FTE-derived ovarian cancer (MOE^{high} - murine oviductal epithelium high passage). *Prl2c2* stable knockdown in MOE^{high} cells demonstrated a significant reduction in cell proliferation, 2-dimensional foci, anchorage independent growth, and blocked tumor formation. The overall survival of ovarian cancer patients from transcriptome analysis of 1868 samples was lower when abundant PRL and prolactin receptors (PRL-R) were expressed. A HGSOC cell line (OVCAR3) and a tumorigenic human FTE cell line (FT33-Tag-Myc) were treated with recombinant PRL and a significant increase in cellular proliferation was detected. A CRISPR/Cas9 mediated PRL-R deletion in OVCAR3 and FT33-Tag-Myc cells demonstrated significant reduction in cell proliferation and eliminated tumor growth using the OVCAR3 model. PRL was found to phosphorylate STAT5, m-TOR and ERK in ovarian cancer cells. This study identified *Prl2c2* as a driver of tumorigenesis in a spontaneous model and confirmed that prolactin signaling supports tumorigenesis in high grade serous ovarian cancer.

Keywords

Prolactin; Prolactin receptor; Spontaneous fallopian tube derived ovarian; cancer model; High grade serous ovarian cancer and p53; phosphorylation

*Corresponding author. 900 S. Ashland (M/C 870), Molecular Biology Research Building Room 3202, Chicago, IL 60607, USA. joannab@uic.edu (J.E. Burdette).

Appendix A. Supplementary data

Supplementary data related to this article can be found at https://doi.org/10.1016/j.canlet.2018.07.003.

Conflicts of interest

The authors have declared that no conflict of interest exists.

1. Introduction

High grade serous ovarian cancer (HGSOC) is the most lethal histotype of ovarian cancer (OVCA) [1], and growing evidence indicates that most HGSOC arises in the fallopian tube epithelium (FTE) [2–4]. Although mouse models with targeted genetic alterations in the FTE (typically called the oviduct in mice) developed HGSOC [5], few models characterize the spontaneous pathogenesis of HGSOC from the fallopian tube, which is essential to identify novel targets of ovarian tumor formation and to understand the disease etiology.

The laying hen has been identified as a spontaneous model of ovarian carcinoma, which develops all four histotypes as humans. While these carcinomas possess similar gene expression profile as seen in humans, it is challenging to study FTE-derived HGSOC in this model, because the oviduct primarily function as a shell gland [6,7]. Spontaneous cellular models of ovarian cancer were previously developed by serially passaging the ovarian surface epithelial (OSE) cells [8]. Using rat OSE cells, the ROSE model was made, which formed ovarian tumors and contained similar recurrent chromosomal alterations to those of OVCA [9]. Two other models of OVCA were derived using murine OSE, called MOSEC and STOSE (spontaneously transformed OSE) [10,11]. Both MOSEC and STOSE formed intraperitoneal tumors. A cDNA microarray on STOSE identified modifications in the expression of several genes that are also modified in HGSOC [10,11]. Although, these models defined the origin and progression of epithelial tumors from the ovary, the spontaneous events that happen in the FTE that can lead to HGSOC remain unexplored.

We previously created a spontaneous model of FTE-derived OVCA by serially passaging murine oviductal epithelial cells (MOE^{high}). These cells formed subcutaneous tumors in mice and transcriptomic analysis of the MOE^{high} cells revealed several pathways that were altered similar to HGSOC such as FOXM1, c-myc, and loss of Cdkn2a [12]. However, several other transcripts were significantly altered that may play an essential role in tumorigenesis of HGSOC, such as *Prl2c2* and *Wnt7b* [12]. *Wnt7b* (Wingless – type MMTV integration site family, member 7B) is a secreted morphogen that was enriched 36-fold in MOE^{high} cells [12]. WNT7B expression levels are enriched in human OVCA and in breast cancer when compared to benign tissues [13,14]. *Prl2c2*, that encodes for proliferin, was amplified > 100 fold in the spontaneous model [12]. Enhanced expression of *Prl2c2* induced malignant transformation of murine fibroblasts and was a critical driver of murine lung adenocarcinoma [15,16]. *Prl2c2* is a murine hormone, without a direct human homolog; however, *Prl2c2* belongs to the prolactin superfamily (prolactin family 2 subfamily c member 2) [17].

Prolactin (PRL) is secreted by the pituitary gland and is best known to stimulate milk production [18]. However, prolactin is also produced locally by many tissues, and increasing evidence supports the hypothesis that the local accumulation of PRL can contribute to tumorigenesis of cancers, such as breast and colorectal [19]. PRL was a component of a multiplex immunoassay called Ovasure, used for early detection of OVCA [20]. While this product is no longer FDA approved, the role of prolactin as a biomarker suggests it might also play a significant role in disease formation and/or progression. Prolactin receptor (PRL-R) activation by its ligand activates several kinases that are well known to stimulate cellular

proliferation [18]. Chronic exposure of PRL induced the transformation of immortalized OSE cells and resulted in tumor formation in mice [19]. Since most human HGSOC are now thought to originate from the FTE, and not the OSE, exploring the signaling mechanism of PRL in human FTE and FTE-like HGSOC cells is necessary.

We hypothesized that *Prl2c2* and *Wnt7b* are critical for enhanced cell proliferation and induction of ovarian tumors in the spontaneous MOE^{high} cells. This study found that both *Wnt7b* and *Prl2c2* were essential for increased cell proliferation of MOE^{high} cells *in vitro,* but only knockdown of *Prl2c2* suppressed MOE^{high} tumors *in vivo.* To translate these findings into human models, the role of PRL and WNT7B signaling in proliferation and tumorigenesis of human FTE and HGSOC cells was explored. Although PRL and WNT7B were sufficient to alter proliferation, PRL alone was pro-tumorigenic in human FTE and tumors, which could have significant implications for future studies aimed at suppressing PRL levels or using neutralizing antibodies to block PRL-R signaling in HGSOC.

2. Materials and methods

2.1. Cell culture

High passage murine oviductal epithelial cells (MOE^{high}) were established as previously described [12]. The human FT33-Tag-Myc cells were a generous gift from Dr. Ronny Drapkin, at the University of Pennsylvania, PA, and were maintained in the media as described earlier [21]. OVCAR3 and OVCAR8 (from ATCC) and OVCAR4 cells (from the National Cancer Institute), were maintained in media as described previously and verified by STR analysis [22].

2.2. Transient transfection and generation of stable cell lines

MOE cells were transiently transfected with pCDNA-Wnt7b (gift from Dr. Marian Waterman, University of California, CA; Addgene plasmid # 35915) [23] using TransIT LT1™ (Mirus Bio, Madison, WI) according to the manufacturer's instructions. For stable cell lines, MOE^{high} cells stably expressing shRNA targeting *Prl2c2*, *Wnt7b*, or a non-target shRNA control were produced by transfecting MOE^{high} cells with shRNA targeting each gene (Supplementary Table S1). FT33-Tag-Myc cells stably expressing a constitutively active PRL-R or empty vector control were produced by transfecting FT33-Tag-Myc cells with pCDNA-PRL-R$_{CA}$ (gift from Dr. Geula Gibori and Dr. Carlos Stocco, University of Illinois at Chicago, IL) and pCMV6-Myc-Neo (donated by Dr. Kwong Wong, M.D. Anderson Cancer Center, Houston, TX). Cell lines were generated by treatment with selection antibiotic and clonal selection. Guide RNAs (gRNA) for CRISPR/Cas9 were designed using CRISPOR (http://crispor.tefor.net/; Supplementary Table 2) [24]. The gRNAs (Integrated DNA Technologies, IA) were cloned into pX330-U6-Chimeric_BB-CBh-hSpCas9 plasmid (gift from Dr. Feng Zhang, Massachusetts Institute of Technology, MA; Addgene plasmid # 42230) [25]. The pX330 plasmid with gRNA was co-transfected with pPGKpuro plasmid (gift from Dr. Rudolf Jaenisch, Massachusetts Institute of Technology, MA; Addgene plasmid # 11349) [26]. Cells were treated with puromycin and single cell clones were isolated. Genomic DNA was extracted from cells using genomic

DNA extraction kit (#G170, Sigma-Aldrich, MO) as per the manufacturer's instructions, and the targeted exon was amplified and sequenced (**primers in** Supplementary Table S2).

2.3. Quantitative reverse transcriptase PCR (qPCR)

RNA was extracted was using Trizol (product # 15596026, Life Technologies, Grand Island, NY) and precipitated with chloroform and isopropanol followed by ethanol washes and DNAse treatment. RNA (1 μg) was reverse transcribed using iScript cDNA synthesis kit (#1708890, Biorad, Hercules, CA) according to manufacturer's instructions. All qPCR measurements were performed using the ABI ViiA7 (Life Technologies, San Diego, CA) and SYBR green (#4913850001, Roche, WI). All qPCR primers (Supplementary Table S3) were validated for specificity by inspection of the melt curve.

2.4. Immunoblotting

Cells were lysed with RIPA buffer (50 mM Tris, pH 7.6, 150 mM NaCl, 1% Triton X-100, 0.1% SDS) containing protease and phosphatase inhibitors (#4693159001, Roche, WI, #P0044, Sigma-Aldrich, St. Louis, MO), freeze-thawed, and centrifuged. Protein (25–30 μg) was separated by electrophoresis in SDS-PAGE gels and transferred to nitrocellulose membrane (#P188018, Thermo Fisher Scientific, Waltham, MA). Blots were then blocked with 5% milk or BSA in TBS-T and probed at 4 °C overnight with primary antibodies (Supplementary Table S4). Membranes were then washed and incubated with HRP-conjugated secondary antibodies raised against rabbit or mouse (#7076 and #7074, Cell Signaling Technology) for 30 min. After washing, membranes were incubated in SuperSignal West Femto substrate (#34095, Thermo Scientific, IL) before imaging on a FlourChem™ E system (ProteinSimple, Santa Clara, CA) [27]. Densitometric analysis was performed using ImageJ (imagej.nih.gov).

2.5. SRB proliferation assay

The sulforhodamine B (SRB) assay was used to measure cell proliferation as previously described [12,28]. Cells (500–25000, depending on cell line) were plated in 96 well plates and incubated for 0, 1, 3, 5 and 7 days. Cells were treated with PRL, small molecule inhibitors, or siRNA. The media was changed after 24 h to media with 2% FBS before the addition of PRL, inhibitors (Supplementary Table S5), or PRL-R siRNA (#EHU095011, Sigma-Aldrich, MO) to each well as indicated. MOE^{High} cells were treated with indicated concentrations of cisplatin for 4 days. Absorbance were read at 505 nm and normalized to its corresponding control (day 0 or vehicle control treatment) to determine relative cell proliferation.

2.6. 2D foci assay

The 2D foci assay was used to measure clonal expansion [12]. Cells were plated (200–500 cells per 60 mm plate), based on cell lines and incubated for 7–15 days according to the growth of cells. After incubation, the cells were fixed with 4% (w/v) paraformaldehyde and then stained with 0.05% crystal violet. Images were taken using FlourChem™ E system (ProteinSimple, Santa Clara, CA). Colonies were counted using ImageJ (imagej.nih.gov).

2.7. Soft agar colony formation for anchorage independent growth

All cells subjected to the soft agar colony formation assay were plated at a density of 15,000 cells/well in a 24-well plate as elucidated previously and cultured for 14 days by replacing fresh media every 5 days [12]. The colonies were imaged using Nikon Eclipse TS100 microscope and counted using ImageJ. Average number of colonies was determined for each well and normalized to control.

2.8. Cell cycle assay

Cells (2×10^6) were seeded in a 10 cm dish and incubated for 24 h. The cells were collected, centrifuged, fixed with 100% ethanol and PBS, stained with propidium iodide, and analyzed using a K2 Cellometer (Nexcelom Biosciences, MA) as per the manufacturer's protocol. Percentage of cells at each stage of the cell cycle was analyzed with the FCS Express program (De Novo Software, Nexcelom Biosciences, MA).

2.9. Animals and xenografts

All animals were treated in accordance with the National Institutes of Health (NIH) Guidelines for the Care and Use of Laboratory Animals and the Institutional Animal Use and Care protocol at the University of Illinois at Chicago (UIC) (protocol 17–174). All mice were housed in a temperature and light controlled environment (12 h light, 12 h dark) and were provided food and water *ad libitum.* For all the cell lines tested, 1×10^6 cells/animal in matrigel were injected subcutaneously into athymic female nude mice. At humane endpoints, all mice were euthanized by CO_2 inhalation followed by cervical dislocation. Tumors were extracted and used for immunohistochemistry analysis.

2.10. Immunohistochemistry (IHC)

Tumors were fixed with 4% paraformaldehyde, dehydrated, and embedded in paraffin. Immunohistochemistry or hematoxylin and eosin stain was performed as described previously [27]. The tissues were deparaffinized and probed with primary antibodies overnight at 4 °C (Supplementary Table S3). The next day, the slides were washed, incubated in secondary antibody conjugated to biotin, and developed with horseradish peroxidase (HRP) and DAB to enable the chromogenic detection of HRP. Tissues that received no primary antibody were used as the negative control. Images were acquired on a Nikon Eclipse E600 microscope using a DS-Ri1 digital camera and NIS Elements software (Nikon Instruments).

2.11. Phosphokinase array

The human phospho-kinase array kit (#ARY003B, R&D systems, MN) was used to identify the proteins that were phosphorylated in response to PRL in OVCAR3 cells. Cell lysis, protein purification, and the assay were performed as per the manufacturer's protocol. Before lysis, the cells were incubated with 10 ng/ml of PRL and 0.1% BSA in PBS (control) for 30 min. Protein (> 500 μg) was used for the analysis and the membranes were imaged on x-ray films (Konica Minolta model: SRX-101A). The mean pixel density of the positive signals that were visually distinct between the control and the PRL treatment were analyzed using ImageJ (imagej.nih.gov).

2.12. Statistical analyses

Data are presented as the mean ± standard error of the mean and represent at least 3 independent biological replicates. Statistical analysis was carried out using GraphPad Prism software (GraphPad, La Jolla, CA). Statistical significance was determined by Student's unpaired t –test, one-way ANOVA, or two-way ANOVA. ANOVAs were followed by with Dunnett's multiple comparison or Tukey's posthoc test. $p < 0.05$ considered significant.

3. Results

3.1. A stable Prl2c2 and Wnt7b knockdown in MOE^{high} cells reduces cell proliferation by accumulating the cells in the G2 phase

In a previous investigation, MOE cells were serially passaged up to 130 passages to generate MOE^{high} cells, resulting in the first spontaneous model of OVCA derived from fallopian tube (murine oviductal) cells [12]. MOE^{high} cells were highly proliferative and formed tumors after subcutaneous xenograft [12]. In that investigation, expression of > 5000 genes were found to be significantly altered compared to the control cells by RNAseq [12]. Of the genes identified as differentially expressed in MOE^{high} cells, a PRL-like gene called *Prl2c2* and *Wnt7b* were chosen for further analysis in the current investigation because they were within the top 10 most enriched genes in MOE^{high} (6.43 and 8.77 $\log_2$ fold increase, respectively), previous studies predicted that these genes were linked to increased cellular proliferation and transformation [13–17], and lastly these targets had not being previously investigated in FTE-derived ovarian cancer [12]. In order to determine if *Prl2c2* or *Wnt7b* were essential for MOE^{high} cell proliferation or transformation, cell lines with stable knockdown (> 50%) using two different shRNA of each gene were generated and validated (Supplementary Figs. S1A–S1F). MOE^{high}/*Prl2c2*$^{shRNA\#1}$ and MOE^{high}/*Prl2c2*$^{shRNA\#2}$ cells displayed a significant reduction in cell proliferation by 65% as compared to a stable non-target shRNA transfected control cells (MOE^{high}/Non-target^{shRNA}) (Fig. 1A). A 2D foci assay measured a significant reduction in the number and the size of foci by 90% in MOE^{high} cells with *Prl2c2* knockdown compared to the control cells (Fig. 1B and Supplementary Fig. S2A). MOE^{high}/*Prl2c2*$^{shRNA\#1}$ and MOE^{high}/*Prl2c2*$^{shRNA\#2}$ cells were also tested in an anchorage independent growth assay. *Prl2c2* knockdown clones had significantly fewer colonies, compared to the control cells (Fig. 1C and Supplementary Fig. S2B). Similarly, *Wnt7b* knockdown significantly reduced MOE^{high} cell proliferation (about 45%) (Fig. 1D), 2D foci counts (70%) (Fig. 1E and Supplementary Fig. S2A) and the number of anchorage independent colonies (Fig. 1F and Supplementary Fig. S2B).

Because *Wnt7b* knockdown did not reduce MOE^{high} proliferation to as great an extent as *Prl2c2* knockdown, *Wnt7b's* effect on cell proliferation was confirmed by transient transfection of *WNT7B* in normal MOE cells (Supplementary Fig. S2C). The cell proliferation was significantly increased at day 3 and day 5 of transfection compared to the vector control (Supplementary Fig. S2D), reiterating the hypothesis that WNT7B enhancement increased the FTE proliferation. These results suggest that *Prl2c2* and *Wnt7b* can individually mediate proliferation in MOE^{high} cells.

To determine if changes in the cell cycle mediated the reduced cell proliferation in *Prl2c2* and *Wnt7b* knockdown cells, propidium iodide staining was performed. Knockdown of *Prl2c2* and *Wnt7b* significantly decreased (50% and 25% respectively) cells in the G1 phase and this correspondingly increased the percentage of cells in the G2 phase compared to MOE^{high} (Fig. 1G and H and Supplementary Fig. S3A). In previous studies, MOE^{high} cells demonstrated increased resistance to chemotherapeutic compounds, including cisplatin [12]. To determine if *Prl2c2* or *Wnt7b* knockdown altered chemosensitivity, the cells were treated with cisplatin in a dose-dependent manner followed by cytotoxicity evaluation. No difference was measured between the knockdown and the control cells (Supplementary Figs. S3B and S3C).

3.2. Prl2c2 reduction in MOE^{high} cells inhibits tumor growth, while Wnt7b suppression did not

Previously, MOE^{high} cells formed tumors within 117 days when injected into the subcutaneous space [12]. To evaluate if *Prl2c2* or *Wnt7b* was essential for tumorigenesis, MOE^{high}/*Prl2c2*$^{shRNA\#1}$ and MOE^{high}/Wnt7b$^{shRNA\#1}$ cells were injected subcutaneously into female athymic nude mice. Both the MOE^{high} and the MOE^{high}/Non-target^{shRNA} cells were injected as controls. All of the mice in the two control groups and *Wnt7b* knockdown formed subcutaneous tumors with no significant difference in the tumor volume (Fig. 2A and B). Interestingly, MOE^{high}/*Prl2c2*$^{shRNA\#1}$ injected mice had no detectable tumors (Fig. 2A and B). At humane endpoints for controls (115 ± 3 days), all mice were sacrificed and IHC analysis was performed on the tumors. Tumors from *Wnt7b* knockdown cells were confirmed to have reduced WNT7B expression compared to tumors from control mice (Supplementary Fig. S4A). H&E staining identified similar spindle-like morphology with same level of intensity of proliferative marker Ki67 and negative CK8 staining as seen in control tumors as previously reported (Supplementary Fig. S4A) [12]. Overall, *Prl2c2* alone, but not *Wnt7b,* was identified as an essential protein for the tumorigenesis of MOE^{high}.

3.3. WNT7B deletion in human HGSOC cells did not reduce tumor growth

Because the murine model still formed tumors with loss of *Wnt7b,* a human model was created to compare the species-specific effect on proliferation and tumor formation. A CRISPR/Cas9 strategy was used to create a *WNT7B* knockout (KO) in OVCAR8^{RFP} (human HGSOC cell line) (Supplementary Fig. S4B and Supplementary Table S6). A significant decrease in cell proliferation by 50% and in the number of 2D foci (70%) was measured in OVCAR8^{RFP}/WNT7B$^{-/-}$ compared to OV-CAR8^{RFP} cells (Fig. 2C and D and Supplementary Fig. S4C). Next, OV-CAR8^{RFP}/WNT7B$^{-/-}$ and OVCAR8^{RFP} cells were injected into the subcutaneous space of the athymic nude mice. As observed previously, OVCAR8^{RFP} cells formed tumors in 35 ± 3 days [22]. At the same time points, OVCAR8^{RFP}/WNT7B$^{-/-}$ also had tumors, and there was no significant difference in the tumor burden over time (Fig. 2E and F). These results confirmed that although *WNT7B* deletion reduced OV-CAR8^{rfp} cell proliferation *in vitro,* it was not sufficient to reduce ovarian tumor burden in murine or human cells.

3.4. Augmentation of prolactin receptors reduces the overall survival of HGSOC patients

The closest homolog of murine *Prl2c2* in human is the hormone prolactin (PRL). To translate the observations obtained using the murine *Prl2c2* model to human PRL and HGSOC, ovarian cancer databases were first analyzed to see if alterations in the ligand (PRL) and its receptors (PRL-R) changed the survival of patients with the disease. Microarray analysis from the Cancer Science Institute of Singapore (CSIOVDB) was used that compared 1868 OVCA samples. The database identified a significant reduction in the overall survival of the OVCA patients with elevated expression of PRL and PRL-R (Fig. 3A and B) [29–31]. The Cancer Genome Atlas (TCGA) provisional database identified an 11% and 13% amplification of PRL-R and PRL, respectively (Supplementary Fig. S5A) [32,33]. Additionally, high accumulation of PRL (117.6 ng/ml) was reported in the serum samples OVCA patients compared to healthy individuals (PRL – 12.5 ng/ml) [19]. A tissue microarray analysis of ovarian tumors contained enriched levels of PRL-R in comparison to normal ovarian epithelial tissue [19]. These analyses indicate that there is a correlation in human samples between high levels of the hormone and receptor and the prevalence and chance of survival for ovarian cancer.

3.5. PRL increases cell proliferation of FT33-Tag-myc and HGSOC cell lines in a dose-dependent manner through PRL-R

PRL production was detected in FT33-Tag-Myc (human FTE cell line, transformed by myc stable expression) [21], and in human HGSOC cell lines including OVCAR3, OVCAR4 and OVCAR8 (Supplementary Fig. S5B). OVCAR3 and FT33-Tag-Myc strongly expressed PRL-R, while OVCAR4 and OVCAR8 had weaker expression (Supplementary Fig. S5B). By treating these cell lines with recombinant human PRL in a dose dependent manner, cell proliferation was analyzed. The proliferation of OVCAR3 and FT33-Tag-Myc cells was significantly and dose dependently enriched after 5 days of PRL exposure, which correlated with higher levels of receptor expression in these cell lines (Fig. 3C). OVCAR8 proliferation significantly increased only at higher doses of PRL, whereas OVCAR4 did not respond to PRL exposure (Fig. 3C), again consistent with both these cell lines having less receptor. Since, PRL increased 2D foci counts in OVCAR3 cells previously [19], a similar analysis with FT33-Tag-Myc cells was tested to directly investigate fallopian tube cells. Recombinant PRL (1 ng/ml) increased the number of foci up to 200%, (Fig. 3D and Supplementary Fig. S5C). A siRNA was used to transiently knockdown PRL-R expression in FT33-Tag-Myc and OVCAR3 cells to confirm if loss of PRL-R mediates changes in proliferation (Supplementary Figs. S5D and S5E). PRL-R knockdown blocked the PRL stimulated cell proliferation (Fig. 3E and F). These results suggest that PRL can induce cell proliferation through its receptor in FTE-derived human cancer cells and in human HGSOC cell lines.

3.6. CRISPR/Cas9-mediated PRL-R knockout blocks FTE cell proliferation, while constitutive activation stimulates FTE proliferation

To identify if changes in the PRL-R levels will affect the human FTE proliferation rate, a plasmid containing constitutively active PRL-R ($_{(PRL\text{-}R_{CA})}$) [34,35] and an empty vector construct (control) were stably transfected into FT33-Tag-Myc cells (Supplementary Fig. S6A). A 30% increase in cell proliferation and 2D foci was detected in the FT33-Tag-Myc/

PRL-R_{CA} clone compared to FT33-Tag-Myc/$Neo^{control}$ cells (Fig. 4A and B and Supplementary Fig. S6B). As further validation, a CRISPR/Cas9-mediated PRL-R KO was made in FT33-Tag-Myc cells (Supplementary Fig. S6C and Supplementary Table S6). A significant reduction in cell proliferation (50%) and in the number of 2D foci (40%) was measured in FT33-Tag-Myc/PRL-$R^{-/-}$ clones as compared to control cells (Fig. 4C and D and Supplementary Fig. S6D). PRL-R activation can augment proliferation and deletion of the receptor blocks proliferation likely due to blocking endogenously produced prolactin signaling.

3.7. PRL-R deletion blocks tumor formation in OVCAR3 cells

Next, to uncover the critical role of PRL-R in HGSOC tumorigenesis, a CRISPR/Cas9-guided PRL-R KO was made in OVCAR3 cells (Supplementary Fig. S6E and Supplementary Table S6). A significant reduction in cell proliferation and 2D foci in $PRLR^{-/-\#1}$ and $PRLR^{-/-\#2}$ cells by > 70% and > 50% respectively was observed (Fig. 4E and F and Supplementary Fig. S6F). OVCAR3 cells form subcutaneous tumors in mice [22]. To evaluate if PRL-R deletion could reduce tumor burden in OVCAR3 cells, OVCAR3/$PRL\text{-}R^{-/-\#1}$, OVCAR3/$PRL\text{-}R^{-/-\#2}$, and parental cells were injected subcutaneously in athymic nude mice. In the control groups, 4/5 of the mice developed tumors at humane endpoints (35 ± 5 days), while no tumors were detected in mice injected with PRL-$R^{-/-}$ clones (Fig. 4G). These findings indicate that PRL-R deletion can significantly inhibit OVCAR3 tumors in mice.

3.8. PRL increases phosphorylation of ERK, AKT, STAT5 and mTOR and small molecule inhibitors block prolactin-mediated proliferation

Although PRL activates multiple pathways in cancer, such as STAT5 and MAPK [18,36], its role in FTE-derived human HGSOC is under-explored. OVCAR3 cells were treated with recombinant prolactin, and the phosphorylation of over 40 kinases was analyzed using a phosphokinase array. MSK½, AKT, TOR, STAT5, p70S6, WNK1, β-catenin, p53 and GSK-3a/b were phosphorylated at critical Ser/Thr/Tyr residues in PRL treated cells compared to the control treatment after 30 min (Fig. 5A and Supplementary Figs. S7A and S7B). Western blotting confirmed, that PRL phosphorylated ERK, STAT5 and mTOR, but not AKT in both OVCAR3 and FT33-Tag-Myc cells within 30 min of exposure (Fig. 5B and C).

To test the importance of PRL signaling on HGSOC proliferation inhibitors for MEK, AKT, STAT5, mTOR, and players in canonical WNT signaling (including β-catenin), were added to OVCAR3 and FT33-Tag-Myc cells with and without PRL. A significant increase in cell proliferation with PRL alone was confirmed compared to the DMSO treated control cells (Fig. 5D and E). The cell proliferation was suppressed by the inhibitors to the level as seen in the control treatment in the presence and absence of PRL (Fig. 5D and E). Interestingly, PRL addition increased the cell proliferation by 1.5-fold in the β-catenin inhibitor treated OVCAR3 and FT33-Tag-Myc cells (Fig. 5D and E). These results reveal activation of key kinases downstream of PRL signaling.

4. Discussion

Overexpression of PRL and its signaling through the PRL-R enhances cell proliferation, colony formation, and tumor formation, while the loss of PRL-R blocks these effects in fallopian tube cell models of cancer and in HGSOC cells. We identified that PRL activates STAT5, m-TOR and MEK and induces cell proliferation in FTE cells. The enhanced expression of PRL homolog, *Prl2c2*, in a murine spontaneous model of fallopian tube-derived cancer led us to investigate PRL in human HGSOC and to confirm its role as a player in ovarian cancer tumorigenesis [12].

Significant attention has focused on evaluating the role of PRL in cancer. Prolactin was part of a six protein panel of proteins used for early detection of ovarian cancer called Ovasure [20], demonstrating that it is specifically increased in tumorigenesis. Recently, PRL was retested along with seven other proteins and found to be an efficient diagnostic marker for screening OVCA with BRCA1 mutation [37]. However, the presence of PRL in the serum does not address if this is a biomarker of cancer or a driver of tumorigenesis. Further, the expression of PRL and its regulation of FTE cells remains relatively unknown. Chronic PRL exposure induced malignant transformation of immortalized OSE cells, which is no longer considered the major progenitor of serous ovarian cancers [19]. Our study focused on FTE – derived OVCA, and used OVCAR3 cells (predicted to be FTE-like) [38]. Although, the protein signature in OVCAR3 cells is similar to FTE cells, it was not completely identical, hence human FTE cells (FT33-Tag-Myc cells) were included [21]. This study found that human FTE actually produce their own PRL as well as many HGSOC cell lines, thus PRL as a biomarker might be a reflection of the fallopian tube origin. In addition to the ligand, MRI or infrared fluorescence imaging bioconjugates were previously designed that specifically bind to the PRL-R [39]. These conjugates effectively underwent selective internalization and facilitated the PRL-R targeted diagnosis of ovarian cancer [39]. Therefore, both the ligand and the receptor of prolactin are not simply biomarkers, but also active drivers of fallopian tube derived HGSOC.

Previously, PRL exposure had been found to activate STAT3, ERK and RAS in gynecological cancer cells [18]. By performing a phosphokinase array with OVCAR3 cells exposed to PRL, phosphorylation of critical proteins including AKT, STAT5, m-TOR, MSK½ and β-catenin was identified. By blocking these kinases in both OVCAR3 and FT33-Tag-Myc cells, it was identified that PRL treatment mainly activated ERK, STAT5 and m-TOR to stimulate cellular proliferation and transformation in human fallopian tube derived tumor cells and in HGSOC cells. Interestingly for HGSOC, which has a deficiency in homologous repair in roughly 50% of patients, PRL accumulation can inhibit the tumor suppressive activity of p21 in breast cancer cells by translocating p-STAT5 into the nucleus and by forming an inhibitory complex with BRCA1 [40]. In the current investigation, the phosphokinase array did not show any change in phosphorylated STAT3 in OVCAR3 cells due to PRL after a 30-min exposure. A previous investigation found that STAT3 phosphorylation was detected after 5 min of PRL exposure [19]. Local accumulation of PRL-amplifies canonical WNT signaling and triggers proliferation in neu-related lipocalin (NRL) – PRL transgenic breast cancer mice models [41]. While, PRL induced phosphorylation of β-catenin in OVCAR3, in the presence of a canonical WNT inhibitor,

PRL induced cell proliferation was not reduced. Intriguingly, we identified novel serine residues in p53 (S15, S46, and S392) that were phosphorylated by PRL exposure. Phosphorylation of these p53 residues had been shown to stabilize the p53 protein and to increase resistance against chemotherapeutics [42]. Future studies should focus on the biological link between PRL and p53 phosphorylation, which may provide novel targets to increase chemosensitivity of ovarian tumors.

The spontaneous FTE derived model mimicked ageing related changes that can occur in women and provided many novel targets, that can be investigated in ovarian cancer pathogenesis [12]. This study selected to evaluate the role of *Prl2c2* and *Wnt7b,* which were both in the top ten significantly modified transcripts in the RNAseq obtained from the spontaneous model. *Prl2c2* was identified to be a critical regulator of cellular proliferation, malignant transformation and tumor growth. In the current study, mice were sacrificed at day 115 based on our previous work with MOE^{high} cells [12]. Importantly, MOE^{high}/ $Prl2c2^{shRNA\#1}$ did not form any tumors, evidencing a clear difference relative to control cells. However, the possibility of tumor development with increased time cannot be ruled out. Although *Prl2c2* is not expressed in humans, it belongs to the PRL family of proteins that share similar structure and function in human reproduction and cancer [43]. Hence, it is important to note that our study relates to human fallopian tube cancer based on PRL, and not *Prl2c2*, which is not in the human genome.

This study also attempted to validate the role of WNT7B in mediating ovarian tumors from the FTE. Our findings revealed that increased WNT7B potentiated cell proliferation *in vitro;* however, both suppression and elimination of WNT7B was not sufficient to block tumor burden in both murine and human ovarian cancer models *in vivo*. All WNTs are secreted proteins and possess high structural similarity [44,45]. We speculate that in the MOE^{high} model, the knockdown of WNT7B could have been rescued by other functional WNTs, such as WNT7A. In the human HGSOC model, the murine WNT7B produced *in vivo* could have restored the functional knockout of human WNT7B in the cell line. Another possibility could be that while WNT7B had a critical function in abnormal cell proliferation and was elevated in malignant cancers, its cellular partner WNT7A may have additional unknown mechanism that could trigger tumor formation. Both MOE^{high} and the human HGSOC models used in this study had high levels of WNT7A. In support of this prediction, an earlier study identified that WNT7A knockdown alone resulted in reduced tumor burden using xenografts of ovarian cancer [14]. WNT7B knockdown may have to be combined with other WNTs suppression in order to reduce ovarian tumor burden and this needs further testing.

Until now, PRL serum levels were only identified as a diagnostic marker for screening OVCA. However, this study for the first time, report that PRL is expressed and mediates tumorigenesis in human FTE. Imaging agents have already been identified to use the receptor to detect tumors *in vivo* [39]. Small molecules were identified to block PRL-R activity and thereby providing a novel strategy, which with further clinical validation, can be used to prevent HGSOC tumor formation from fallopian tube.

Supplementary Material

Refer to Web version on PubMed Central for supplementary material.

Acknowledgements

We thank UIC Research Resources Center Genome Editing Core for their intellectual contribution in CRISPR/Cas9 technique.

Financial support

UIC Multi-Disciplinary Chancellor Fellowship, UIC Dean Scholar Fellowship, Ann and Sol Schreiber Ovarian Cancer Research Fund Alliance Postdoctoral Award 543296, NIH NIEHS UG3 ES029073, and the Tell Every Amazing Lady TEALWALK Award.

Abbreviations:

HGSOC	High grade serous ovarian cancer
FTE	Fallopian tube epithelium
MOE	Murine oviductal epithelium
PRL	Prolactin
PRL-R	Prolactin receptors

References

[1]. Seidman JD, Horkayne-Szakaly I, Haiba M, Boice CR, Kurman RJ, Ronnett BM, The histologic type and stage distribution of ovarian carcinomas of surface epithelial origin, Int. J. Gynecol. Pathol. Official J. Int. Soc. Gynecol. Pathol. 23 (2004) 41–44.

[2]. Auersperg N, The origin of ovarian cancers–hypotheses and controversies, Front Biosci (Schol Ed) 5 (2013) 709–719. [PubMed: 23277080]

[3]. Marquez RT, Baggerly KA, Patterson AP, Liu J, Broaddus R, Frumovitz M, Atkinson EN, Smith DI, Hartmann L, Fishman D, Berchuck A, Whitaker R, Gershenson DM, Mills GB, Bast RC Jr., Lu KH, Patterns of gene expression in different histotypes of epithelial ovarian cancer correlate with those in normal fallopian tube, endometrium, and colon, Clin. Canc. Res. Official J. Am. Assoc. Canc. Res. 11 (2005) 6116–6126.

[4]. Merritt MA, Bentink S, Schwede M, Iwanicki MP, Quackenbush J, Woo T, Agoston ES, Reinhardt F, Crum CP, Berkowitz RS, Mok SC, Witt AE, Jones MA, Wang B, Ince TA, Gene expression signature of normal cell-of-origin predicts ovarian tumor outcomes, PLoS One 8 (2013) e80314.

[5]. Perets R, Wyant GA, Muto KW, Bijron JG, Poole BB, Chin KT, Chen JY, Ohman AW, Stepule CD, Kwak S, Karst AM, Hirsch MS, Setlur SR, Crum CP, Dinulescu DM, Drapkin R, Transformation of the fallopian tube secretory epithelium leads to high-grade serous ovarian cancer in Brca;Tp53;Pten models, Canc Cell 24 (2013) 751–765.

[6]. Barua A, Bitterman P, Abramowicz JS, Dirks AL, Bahr JM, Hales DB, Bradaric MJ, Edassery SL, Rotmensch J, Luborsky JL, Histopathology of ovarian tumors in laying hens: a preclinical model of human ovarian cancer, Int. J. Gynecol. Canc 19 (2009) 531–539.

[7]. Johnson PA, Giles JR, The hen as a model of ovarian cancer, Nat. Rev. Canc 13 (2013) 432–436.

[8]. Garson K, Shaw TJ, Clark KV, Yao DS, Vanderhyden BC, Models of ovarian cancer-are we there yet? Mol. Cell. Endocrinol. 239 (2005) 15–26. [PubMed: 15955618]

[9]. Testa JR, Getts LA, Salazar H, Liu Z, Handel LM, Godwin AK, Hamilton TC, Spontaneous transformation of rat ovarian surface epithelial cells results in well to poorly differentiated tumors with a parallel range of cytogenetic complexity, Canc. Res. 54 (1994) 2778–2784.

[10]. Roby KF, Taylor CC, Sweetwood JP, Cheng Y, Pace JL, Tawfik O, Persons DL, Smith PG, Terranova PF, Development of a syngeneic mouse model for events related to ovarian cancer, Carcinogenesis 21 (2000) 585–591. [PubMed: 10753190]

[11]. McCloskey CW, Goldberg RL, Carter LE, Gamwell LF, Al-Hujaily EM, Collins O, Macdonald EA, Garson K, Daneshmand M, Carmona E, Vanderhyden BC, A new spontaneously transformed syngeneic model of high-grade serous ovarian cancer with a tumor-initiating cell population, Front Oncol. 4 (2014) 53. [PubMed: 24672774]

[12]. Endsley MP, Moyle-Heyrman G, Karthikeyan S, Lantvit DD, Davis DA, Wei JJ, Burdette JE, Spontaneous transformation of murine oviductal epithelial cells: a model system to investigate the onset of fallopian-derived tumors, Front Oncol. 5 (2015) 154. [PubMed: 26236688]

[13]. Huguet EL, McMahon JA, McMahon AP, Bicknell R, Harris AL, Differential expression of human Wnt genes 2, 3, 4, and 7B in human breast cell lines and normal and disease states of human breast tissue, Canc. Res. 54 (1994) 2615–2621.

[14]. Yoshioka S, King ML, Ran S, Okuda H, MacLean JA 2nd , McAsey ME, Sugino N, Brard L, Watabe K, Hayashi K, WNT7A regulates tumor growth and progression in ovarian cancer through the WNT/beta-catenin pathway, Mol. Canc. Res. MCR 10 (2012) 469–482.

[15]. Parfett CL, Induction of proliferin gene expression by diverse chemical agents that promote morphological transformation in C3H/10T½ cultures, Canc. Lett. 64 (1992) 1–9.

[16]. Kanellakis NI, Giannou A, Pepe M, Agalioti T, Zazara D, Vreka M, Lilis I, Giopanou I, Spella M, Marazioti A, Rahman N, Pavord I, Psallidas I, Stathopoulos GT, Mouse lung adenocarcinoma cell lines reveal Prl2c2 as a novel lung tumour promoter, Thorax 71 (2016) A7–A7.

[17]. Missan DS, Chittur SV, DiPersio CM, Regulation of fibulin-2 gene expression by integrin alpha3beta1 contributes to the invasive phenotype of transformed keratinocytes, J. Invest. Dermatol. 134 (2014) 2418–2427. [PubMed: 24694902]

[18]. Bernard V, Young J, Chanson P, Binart N, New insights in prolactin: pathological implications, Nat. Rev. Endocrinol. 11 (2015) 265–275. [PubMed: 25781857]

[19]. Levina VV, Nolen B, Su Y, Godwin AK, Fishman D, Liu J, Mor G, Maxwell LG, Herberman RB, Szczepanski MJ, Szajnik ME, Gorelik E, Lokshin AE, Biological significance of prolactin in gynecologic cancers, Canc. Res. 69 (2009) 5226–5233.

[20]. Buchen L, Cancer: missing the mark, Nature 471 (2011) 428–432. [PubMed: 21430749]

[21]. Karst AM, Levanon K, Drapkin R, Modeling high-grade serous ovarian carcinogenesis from the fallopian tube, Proc. Natl. Acad. Sci. U. S. A. 108 (2011) 7547–7552. [PubMed: 21502498]

[22]. Mitra AK, Davis DA, Tomar S, Roy L, Gurler H, Xie J, Lantvit DD, Cardenas H, Fang F, Liu Y, Loughran E, Yang J, Sharon Stack M, Emerson RE, Cowden Dahl KD, M VB, Nephew KP, Matei D, Burdette JE, In vivo tumor growth of high-grade serous ovarian cancer cell lines, Gynecol. Oncol. 138 (2015) 372–377. [PubMed: 26050922]

[23]. Najdi R, Proffitt K, Sprowl S, Kaur S, Yu J, Covey TM, Virshup DM, Waterman ML, A uniform human Wnt expression library reveals a shared secretory pathway and unique signaling activities, Differentiation 84 (2012) 203–213. [PubMed: 22784633]

[24]. Haeussler M, Schonig K, Eckert H, Eschstruth A, Mianne J, Renaud JB, Schneider-Maunoury S, Shkumatava A, Teboul L, Kent J, Joly JS, Concordet JP, Evaluation of off-target and on-target scoring algorithms and integration into the guide RNA selection tool CRISPOR, Genome Biol. 17 (2016) 148. [PubMed: 27380939]

[25]. Cong L, Ran FA, Cox D, Lin SL, Barretto R, Habib N, Hsu PD, Wu XB, Jiang WY, Marraffini LA, Zhang F, Multiplex genome engineering using CRISPR/Cas systems, Science 339 (2013) 819–823. [PubMed: 23287718]

[26]. Tucker KL, Beard C, Dausman T, JacksonGrusby L, Laird PW, Lei H, Li E, Jaenisch R, Germ-line passage is required for establishment of methylation and expression patterns of imprinted but not of nonimprinted genes, Genes Dev. 10 (1996) 1008–1020. [PubMed: 8608936]

[27]. Karthikeyan S, Lantvit DD, Chae DH, Burdette JE, Cadherin-6 type 2, K-cadherin (CDH6) is regulated by mutant p53 in the fallopian tube but is not expressed in the ovarian surface, Oncotarget 7 (2016) 69871–69882. [PubMed: 27563818]

[28]. Dean M, Davis DA, Burdette JE, Activin A stimulates migration of the fallopian tube epithelium, an origin of high-grade serous ovarian cancer, through non-canonical signaling, Canc. Lett. 391 (2017) 114–124.

[29]. Tan TZ, Yang H, Ye J, Low J, Choolani M, Tan DS, Thiery JP, Huang RY, CSIOVDB: a microarray gene expression database of epithelial ovarian cancer subtype, Oncotarget 6 (2015) 43843–43852. [PubMed: 26549805]

[30]. Tan TZ, Miow QH, Huang RY, Wong MK, Ye J, Lau JA, Wu MC, Bin Abdul Hadi LH, Soong R, Choolani M, Davidson B, Nesland JM, Wang LZ, Matsumura N, Mandai M, Konishi I, Goh BC, Chang JT, Thiery JP, Mori S, Functional genomics identifies five distinct molecular subtypes with clinical relevance and pathways for growth control in epithelial ovarian cancer, EMBO Mol. Med. 5 (2013) 1051–1066. [PubMed: 23666744]

[31]. Tan TZ, Miow QH, Miki Y, Noda T, Mori S, Huang RY, Thiery JP, Epithelial-mesenchymal transition spectrum quantification and its efficacy in deciphering survival and drug responses of cancer patients, EMBO Mol. Med. 6 (2014) 1279–1293. [PubMed: 25214461]

[32]. Gao J, Aksoy BA, Dogrusoz U, Dresdner G, Gross B, Sumer SO, Sun Y, Jacobsen A, Sinha R, Larsson E, Cerami E, Sander C, Schultz N, Integrative analysis of complex cancer genomics and clinical profiles using the cBioPortal, Sci. Signal 6 (2013) l1.

[33]. Cerami E, Gao J, Dogrusoz U, Gross BE, Sumer SO, Aksoy BA, Jacobsen A, Byrne CJ, Heuer ML, Larsson E, Antipin Y, Reva B, Goldberg AP, Sander C, Schultz N, The cBio cancer genomics portal: an open platform for exploring multidimensional cancer genomics data, Canc. Discov. 2 (2012) 401–404.

[34]. Frasor J, Barkai U, Zhong L, Fazleabas AT, Gibori G, PRL-induced ERalpha gene expression is mediated by Janus kinase 2 (Jak2) while signal transducer and activator of transcription 5b (Stat5b) phosphorylation involves Jak2 and a second tyrosine kinase, Mol. Endocrinol. 15 (2001) 1941–1952. [PubMed: 11682625]

[35]. Stocco C, Djiane J, Gibori G, Prostaglandin F(2alpha) (PGF(2alpha)) and prolactin signaling: PGF(2alpha)-mediated inhibition of prolactin receptor expression in the Corpus luteum, Endocrinology 144 (2003) 3301–3305. [PubMed: 12865306]

[36]. Goffin V, Prolactin receptor targeting in breast and prostate cancers: new insights into an old challenge, Pharmacol. Ther. 179 (2017) 111–126. [PubMed: 28549597]

[37]. Gschwantler-Kaulich D, Weingartshofer S, Rappaport-Furhauser C, Zeilinger R, Pils D, Muhr D, Braicu EI, Kastner MT, Tan YY, Semmler L, Sehouli J, Singer CF, Diagnostic markers for the detection of ovarian cancer in BRCA1 mutation carriers, PLoS One 12 (2017) e0189641.

[38]. Coscia F, Watters KM, Curtis M, Eckert MA, Chiang CY, Tyanova S, Montag A, Lastra RR, Lengyel E, Mann M, Integrative proteomic profiling of ovarian cancer cell lines reveals precursor cell associated proteins and functional status, Nat. Commun 7 (2016) 12645. [PubMed: 27561551]

[39]. Sundaram KM, Zhang Y, Mitra AK, Kouadio JK, Gwin K, Kossiakoff AA, Roman BB, Lengyel E, Piccirilli JA, Prolactin receptor-mediated internalization of imaging agents detects epithelial ovarian cancer with enhanced sensitivity and specificity, Canc. Res 77 (2017) 1684–1696.

[40]. Chen KE, Walker AM, Prolactin inhibits a major tumor-suppressive function of wild type BRCA1, Canc. Lett. 375 (2016) 293–302.

[41]. O'Leary KA, Shea MP, Salituro S, Blohm CE, Schuler LA, Prolactin alters the mammary epithelial hierarchy, increasing progenitors and facilitating ovarian steroid action, Stem Cell Rep. 9 (2017) 1167–1179.

[42]. Thompson T, Tovar C, Yang H, Carvajal D, Vu BT, Xu Q, Wahl GM, Heimbrook DC, Vassilev LT, Phosphorylation of p53 on key serines is dispensable for transcriptional activation and apoptosis, J. Biol. Chem. 279 (2004) 53015–53022. [PubMed: 15471885]

[43]. Lopez Vicchi F, Becu-Villalobos D, Prolactin: the bright and the dark side, Endocrinology 158 (2017) 1556–1559. [PubMed: 28575433]

[44]. Nusse R, Clevers H, Wnt/beta-Catenin signaling, disease, and emerging therapeutic modalities, Cell 169 (2017) 985–999. [PubMed: 28575679]

[45]. Arend RC, Londono-Joshi AI, Straughn JM Jr., Buchsbaum DJ, The Wnt/beta-catenin pathway in ovarian cancer: a review, Gynecol. Oncol. 131 (2013) 772–779. [PubMed: 24125749]

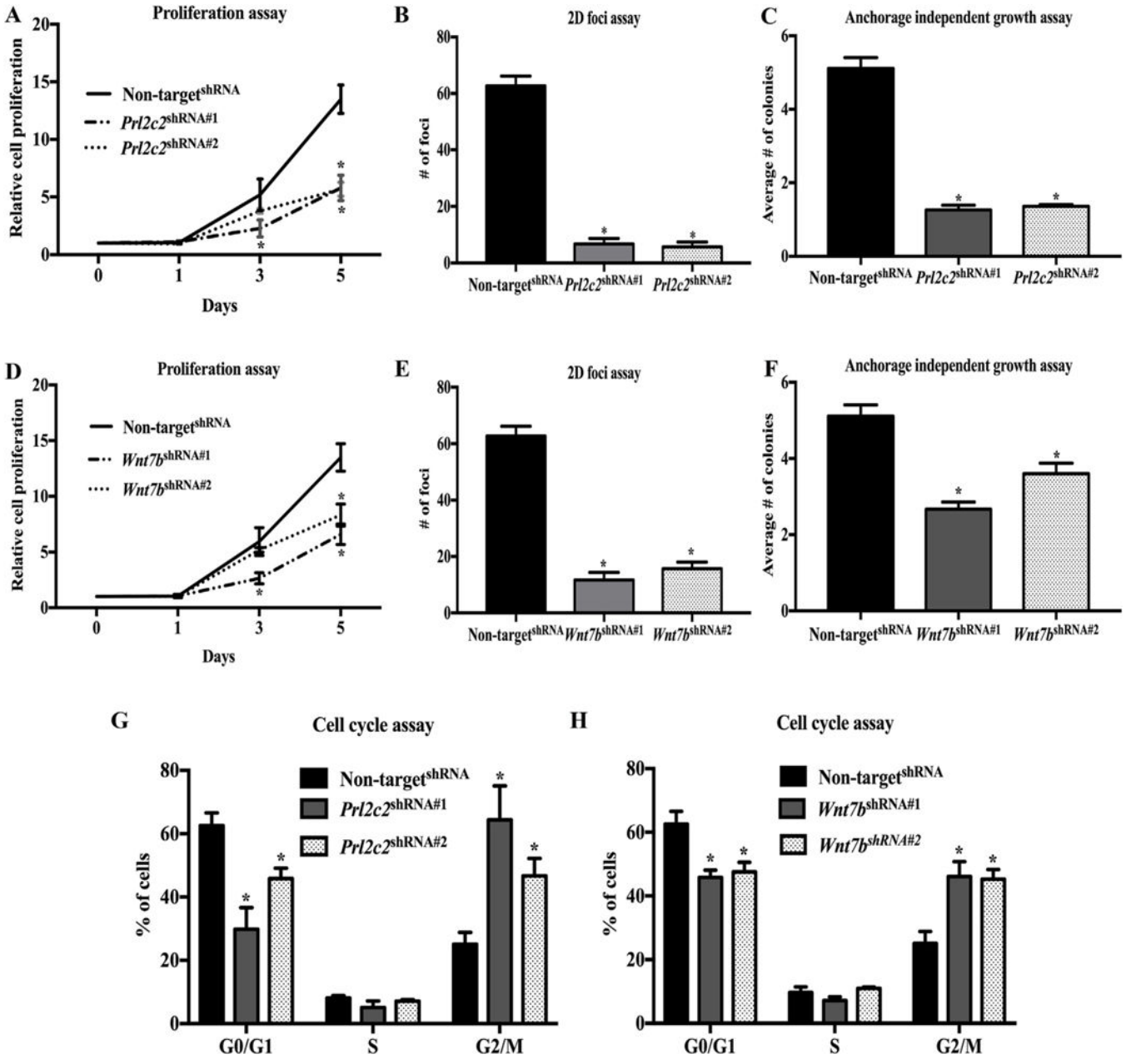

Fig. 1. *PrI2c2* and *Wnt7b* knockdown reduces cell proliferation of MOE^{high} cells.

A & D. SRB assay measured cell proliferation with *Prl2c2* or *Wnt7b* knockdown over days. B & E. 2D foci assay quantified the number of foci on day 7 after plating. C & F. Anchorage independent colonies were quantified using soft agar assay in MOE^{high} clones. G &H. Cell cycle analysis of MOE^{high} cells with *Prl2c2, Wnt7b* knockdown and non-target^{shRNA} control cells. Data are represented as mean ± SEM (n ≥ 5). *, $p < 0.05$ relative to MOE^{high}/Non-target^{shRNA} cells.

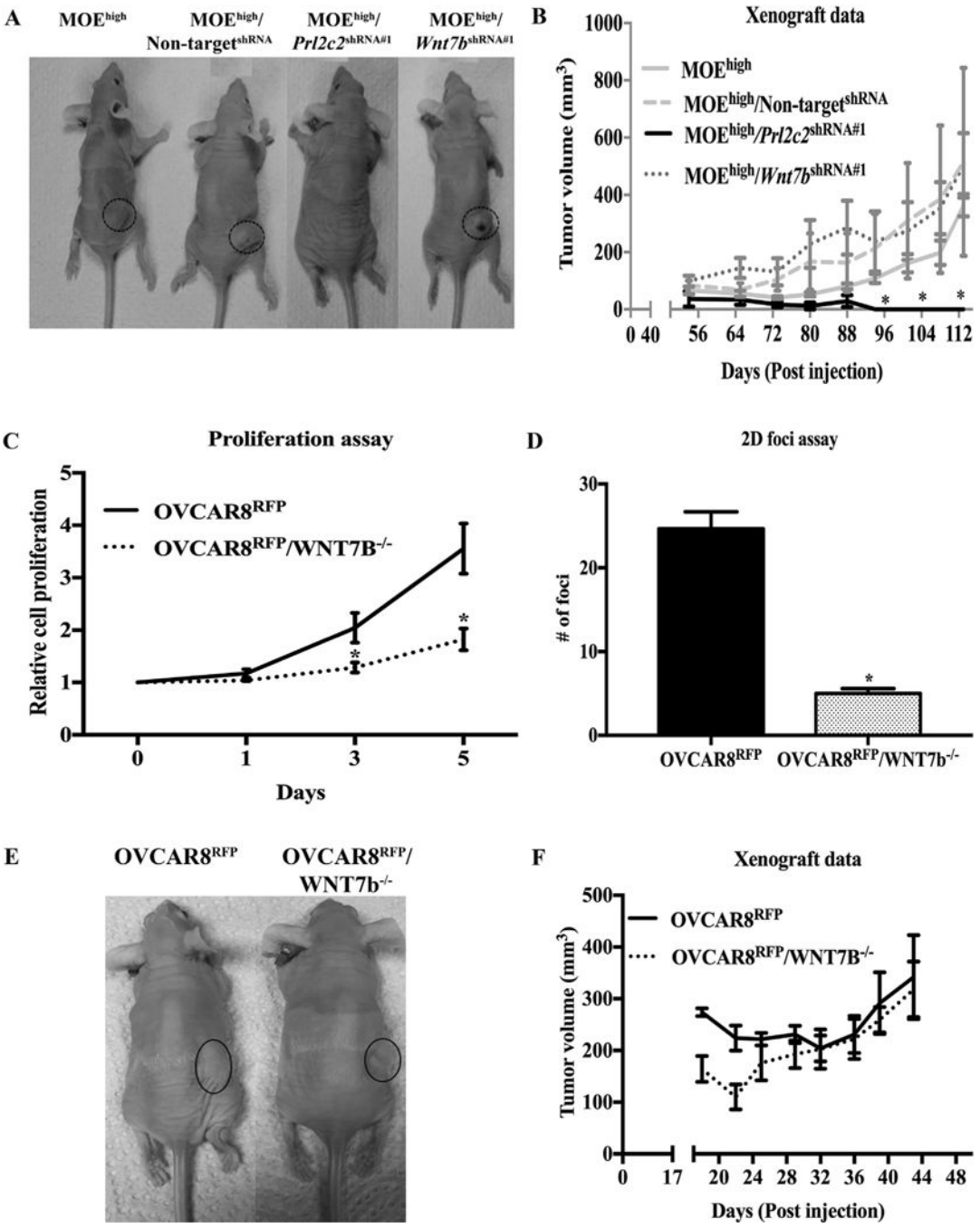

Fig. 2. *Prl2c2* knockdown blocks tumor formation in MOE^{high} cells, while both *Wnt7b* knockdown and deletion do not alter ovarian tumor burden.

A.Representative picture of athymic nude mice bearing tumors after xenograft with MOE^{high} clones. Black circle indicates the subcutaneous tumor. MOE^{high} (n = 3), MOE^{high}/Non-target^{shRNA} (n = 3), MOE^{high}/*Prl2c2*$^{shRNA\#1}$ (n = 5), MOE^{high}/Wnt7b$^{shRNA\#1}$ (n = 5). B. Tumor volume measured with calipers of MOE^{high} clones over time. C. SRB assay measured cell proliferation of OVCAR8^{RFP}/*WNT7B*$^{-/-}$. D. 2D foci assay quantified the number of foci. E. Picture with OVCAR8^{RFP} xenografts. Black circle indicates the tumor growth. OVCAR8^{RFP} (n = 3), OVCAR8^{RFP}/*WNT7B*$^{-/-}$ (n = 5). F. Tumor volume measured

with calipers of OVCAR8^{RFP} and OVCAR8^{RFP}/*WNT7B*$^{-/-}$ over time. Data are represented as mean ± SEM (n ≥ 3). *, $p < 0.05$ relative to MOE^{high}/Non-target^{shRNA} cells or OVCAR8 cells.

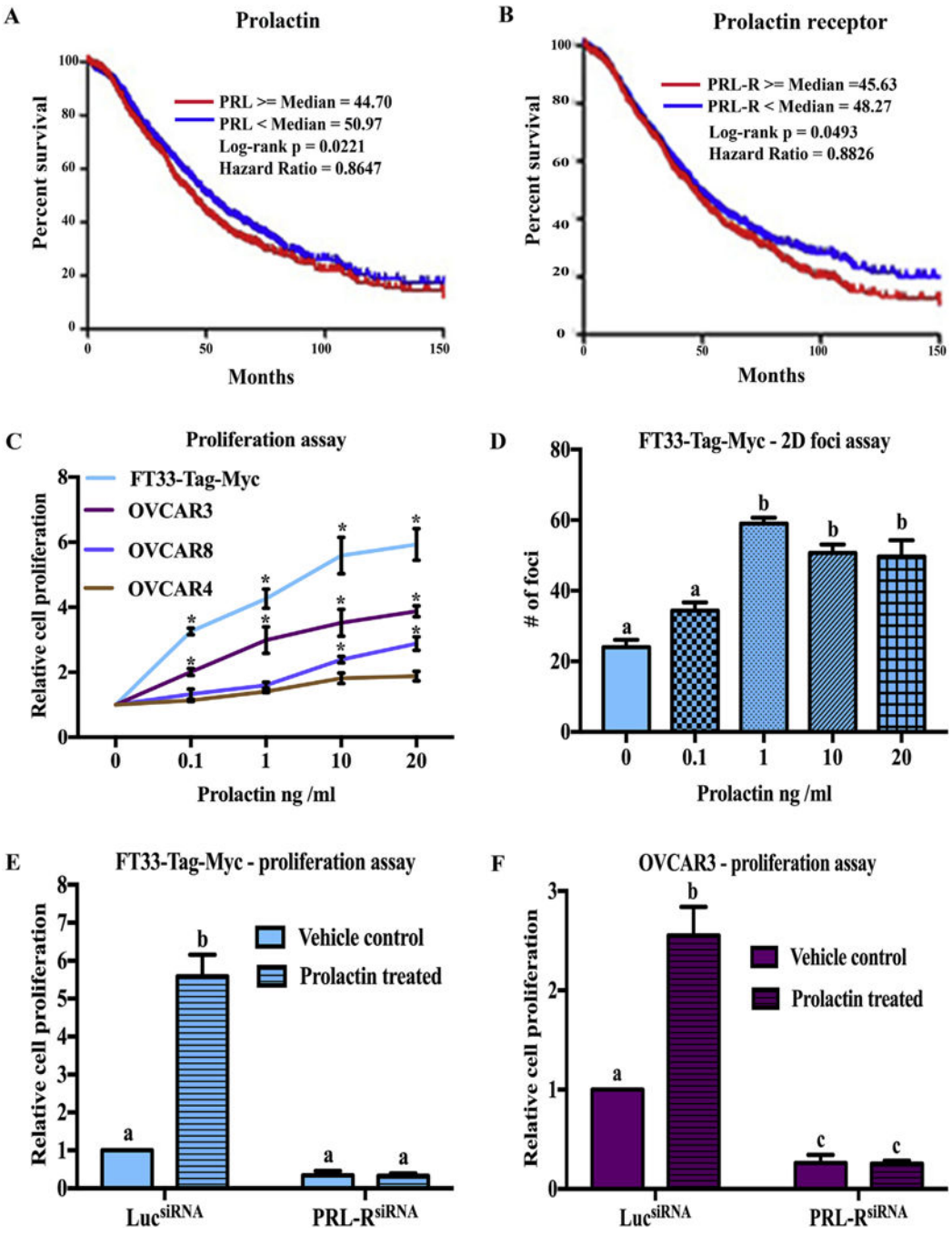

Fig. 3. PRL and PRL-R triggers cell proliferation and its expression is correlated with overall survival.

A &B. Overall survival from CSIOVDB databases with enhanced expression of PRL and PRL-R. *p* values were obtained for comparison between any two groups, log-rank test. C. Cell proliferation data obtained by SRB assay on day 5 of PRL treatment. D. 2D foci of FT33-Tag-Myc cells on day 15 of PRL exposure. PRL-R expression was transiently reduced using siRNA. After 24h of transfection, PRL was added at a concentration of 10 ng/ml and SRB assay was performed with FT33-Tag-Myc cells (E) or OVCAR3 cells (F). Data are represented as mean ± SEM (n ≥ 3). *, $p < 0.05$ and bars without common superscript are

significantly different ($p < 0.05$) relative to vehicle control treatment or Luc^{siRNA} transfection.

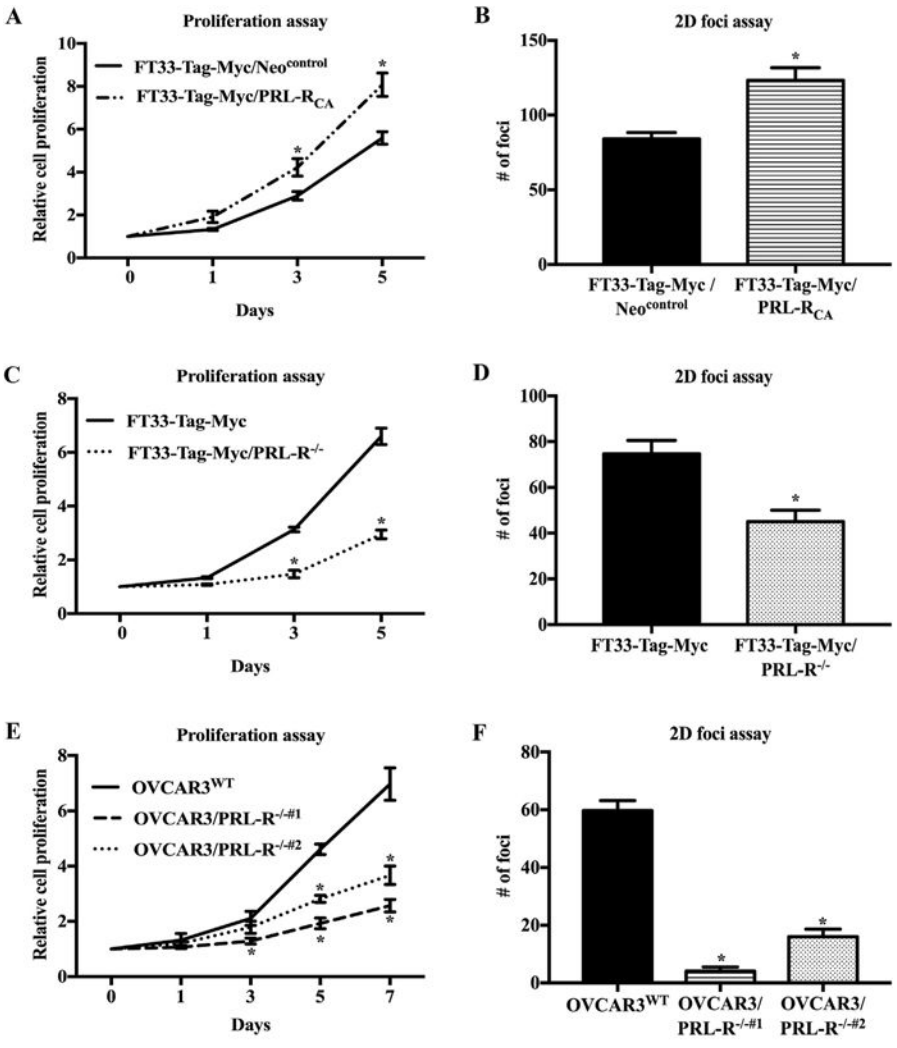

G OVCAR3 xenograft

S.No	Cell line	Tumor take
1	OVCAR3^{WT}	4/5
2	OVCAR3/PRLR$^{-/-\#1}$	0/5
3	OVCAR3/PRLR$^{-/-\#2}$	0/5

Fig. 4. CRISPR/Cas9 mediated PRL-R KO blocks cell proliferation in human FTE and tumor formation in HGSOC cells.

A. SRB assay measured the cell proliferation over time. B. 2D foci assay graph with quantified number of foci in FT33-Tag-Myc/PRL-R_{CA} (constitutively active) clone and vector control. C. Relative cell proliferation was measured by SRB assay on FT-33-Tag-Myc and FT33-Tag-Myc/PRL-$R^{-/-}$ clone over days. D. 2D foci assay graph with quantified number of foci in FT33-Tag-Myc/PRL-$R^{-/-}$ clone and control. E. Cell proliferation data of OVCAR3 cells control and PRL-$R^{-/-}$ clones. F. 2D foci assay after 15 days. G. Table

indicating the tumor take rate in OVCAR3 xenografts models. Data are represented as mean ± SEM (n ≥ 5). *, $p < 0.05$ relative to control cells.

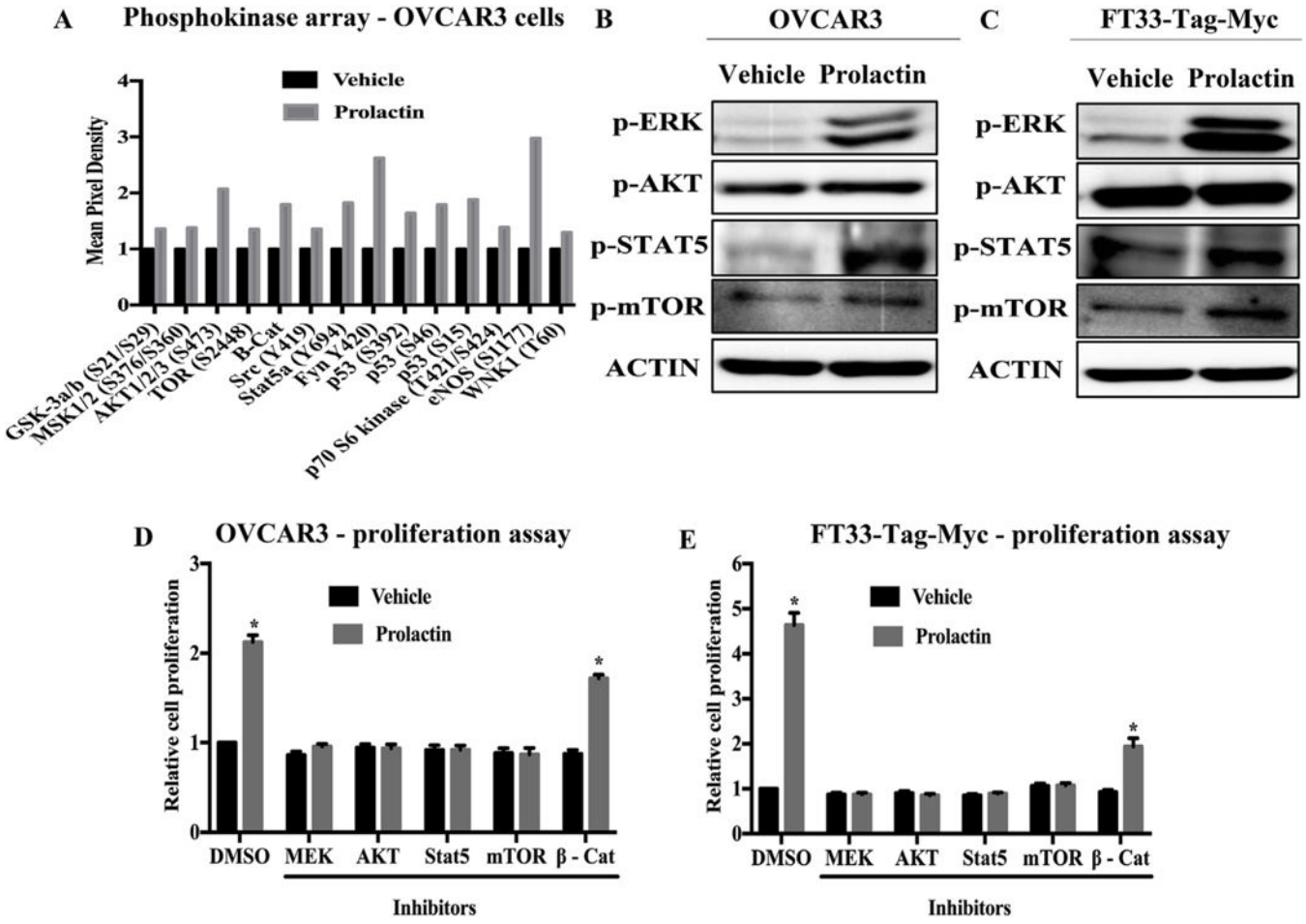

Fig. 5. PRL exposure induces phosphorylation of many growth pathways in human FTE and FTE-derived HGSOC cells.

A. Human phosphokinase array identified phosphorylated proteins in OVCAR3 cells with 30 min of PRL treatment. B & C. Western blotting confirmed the phosphorylated proteins post 30 min of PRL treatment. D & E. SRB assay measured cell proliferation changes with PRL and inhibitors. Data are represented as mean ± SEM (n ≥ 3). *, $p < 0.05$ relative to control.